ENVIRONMENTAL RESEARCH
LETTERS

LETTER • OPEN ACCESS

Role of multi-decadal variability of the winter North Atlantic Oscillation on Northern Hemisphere climate

To cite this article: Andrew P Schurer *et al* 2023 *Environ. Res. Lett.* **18** 044046

ENVIRONMENTAL RESEARCH
LETTERS

OPEN ACCESS

RECEIVED
25 January 2023

REVISED
6 March 2023

ACCEPTED FOR PUBLICATION
15 March 2023

PUBLISHED
17 April 2023

LETTER

Role of multi-decadal variability of the winter North Atlantic Oscillation on Northern Hemisphere climate

Andrew P Schurer[1,*], Gabriele C Hegerl[1], Hugues Goosse[2], Massimo A Bollasina[1], Matthew H England[3], Doug M Smith[4] and Simon F B Tett[1]

[1] School of GeoSciences, University of Edinburgh, Edinburgh EH9, United Kingdom
[2] Université Catholique de Louvain, Earth and Life Institute, Louvain-La-Neuve, Belgium
[3] Climate Change Research Centre, University of New South Wales, Sydney NSW 2052, Australia
[4] Met Office Hadley Centre, Exeter, United Kingdom
[*] Author to whom any correspondence should be addressed.

E-mail: a.schurer@ed.ac.uk

Keywords: multi-decadal, Atlantic, climate variability, North Atlantic Oscillation

Supplementary material for this article is available online

Abstract

The North Atlantic Oscillation (NAO) plays a leading role in modulating wintertime climate over the North Atlantic and the surrounding continents of Europe and North America. Here we show that the observed evolution of the NAO displays larger multi-decadal variability than that simulated by nearly all CMIP6 models. To investigate the role of the NAO as a pacemaker of multi-decadal climate variability, we analyse simulations that are constrained to follow the observed NAO. We use a particle filter data-assimilation technique that sub-selects members that follow the observed NAO among an ensemble of simulations, as well as the El Niño Southern Oscillation and Southern Annular Mode in a global climate model, without the use of nudging terms. Since the climate model also contains external forcings, these simulations can be used to compare the simulated forced response to the effect of the three assimilated modes. Concentrating on the 28 year periods of strongest observed NAO trends, we show that NAO variability leads to large multi-decadal trends in temperature and precipitation over Northern Hemisphere land as well as in sea-ice concentration. The Atlantic subpolar gyre region is particularly strongly influenced by the NAO, with links found to both concurrent atmospheric variability and to the Atlantic Meridional Overturning Circulation (AMOC). Care thus needs to be taken to account for impacts of the NAO when using sea surface temperature in this region as a proxy for AMOC strength over decadal to multi-decadal time-scales. Our results have important implications for climate analyses of the North Atlantic region and highlight the need for further work to understand the causes of multi-decadal NAO variability.

1. Introduction

The North Atlantic Oscillation (NAO) is the leading mode of atmospheric variability over the North Atlantic, characterised by a pressure gradient between Iceland and the Azores. The NAO exerts a dominant influence on wintertime temperature, precipitation, storms and sea-ice cover [1]. A positive mode of the NAO is associated with more Atlantic storms, a warmer and wetter Northern Europe, and a drier Mediterranean, with an opposite climatic effect during its negative phase. Several studies have found an important role for the NAO in decadal climate trends, particularly at mid-high latitudes in the Northern Hemisphere [2–4]. Long-term variability in the annular modes (which includes the NAO in the Northern Hemisphere and the Southern Annular Mode (SAM) in the Southern Hemisphere) has also been found to be a primary source of uncertainty in climate projections in the mid and high-latitudes

[5]. The important role of the NAO on Northern Hemisphere climate has led to considerable interest in its predictability in decadal forecasts [6]. Long-term variability of the NAO has also been found to influence ocean dynamics, with positive phases of the NAO leading to a strengthening of the Atlantic Meridional Overturning Circulation (AMOC) [7], with possible links to the Atlantic Multidecadal Variability (AMV) [8].

Several recent studies have found inconsistencies between the observed large scale North Atlantic atmospheric circulation variability and that simulated by climate models. In particular, it has been found that climate models underestimate observed long-term variability in the North Atlantic, as characterised by variability in the NAO and North Atlantic jet stream on multi-decadal scales [9, 10]. The explanation behind this apparent discrepancy is still an active topic of research, with several studies suggesting that models may not be simulating the correct link between sea surface temperature (SST) and the jet stream [11–13], while others find that the discrepancy could be due to deficient stratospheric [14], and/or tropospheric [15] dynamics, or that much of this discrepancy could be due to external forcings [6]. O'Reilly *et al* [16] investigated the importance of the lack of simulated atmospheric variability on predicted 21st Century climate, finding that the uncertainty in projections of temperature and precipitation over much of the northern extratropics is often underestimated.

Here, we use a particle filter model experiment to investigate the effect that multi-decadal variability of the NAO likely had on wintertime climate during the 20th Century. The model simulations are constrained to align with the observed evolution of the El Niño Southern Oscillation (ENSO), SAM and NAO variability throughout the simulation period. In this paper we concentrate exclusively on the effect of the NAO, with the effect of the other two modes assimilated minimized by concentrating on periods of strong NAO trends, as well as variables and areas where the effects of the other modes are expected to be small. A comparison with simulated variables in unconstrained models in these regions, such as Northern Hemisphere temperature and precipitation, sea ice, and Atlantic variability, allows the impact of this mode of variability to be assessed. The experimental setup is described in section 2, in addition to the observations used, and the analysis methods employed. The results of the simulations are discussed in section 3 where the role of the NAO on long-term climate variability is investigated and the link to the AMOC explored. The paper concludes with a discussion of the significance of the results and a brief summary in section 4.

2. Data and methods

2.1. Observations

The instrumental datasets used in the analysis presented in this paper are as follows; HadCRUT5 for surface air temperature (SAT) [17], and HadSST4 for SST [18]. The 20th Century reanalysis version 3 [19] is employed for sea level pressure (SLP) and HadISST2 [20] for sea-ice cover. Lastly, GPCC is used for precipitation [21].

2.2. Model experiments

We analyse a set of experiments with the coupled atmosphere-ocean model HadCM3 [22, 23]. These include: a pre-industrial control (*piControl*) simulation with no time-varying external forcings [24]. A ten-member ensemble with all CMIP5 external forcings covering the period 1780–2008 (*Hist)* [25, 26] (for two variables: AMOC and sea-ice cover, only 9-members are available due to a data-processing error). The particle filter simulations for 1780–2008 (*Hist-assim*) [27, 28]. A number of ensembles forced with individual forcings covering the period 1400–2000, including 4 simulations with only greenhouse gas forcing (*GHG*), 3 with only volcanic forcing (*VOLC*) [24] and the response to anthropogenic aerosols (*AER*), estimated by calculating the difference between simulations with all forcings and those with all forcings except aerosols [24].

Hist-assim uses the same forcings as the *Hist* simulations but has the evolution of the index of three modes of variability (i.e. ENSO, SAM and NAO) constrained to be close to those observed. Full details of the particle filter set-up can be found in Schurer *et al* [27] and is based on the technique described in [29, 30]. In this implementation 50 simulations (or particles) are run for a year at which point the assimilation retains those which are consistent with the assimilated observations, namely the Niño 3.4 ENSO index, the Marshall SAM index and a station based NAO index, defined following Luterbacher *et al* [31]. The same number of simulations [32] are then run for the next year with initial conditions preferentially taken from the simulations which better match the observed variability of the preceding year, so that those that are most consistent with the observations provide starting conditions for multiple new simulations and those which are least consistent are stopped. The result is a probabilistic distribution of the simulated variables at each time step as well as a single continuous simulation (*Hist-assim*) whose modes of variability are close to those observed (figure S1). Given that the experimental setup does not include any nudging terms, none of simulations can perfectly match all three assimilated indices simultaneously. How close the filter tracks each index is determined by the relative uncertainty of each of the observed indices assimilated. For most of the experiment the filter tracks the NAO very closely, however towards the end of the 20th century the fit degrades slightly, as the observations of the SAM and ENSO become more certain [27]. We therefore focus our analysis on the period of close alignment (before 1990).

2.3. Analysis methods

To assess the importance of the NAO, trends in winter (December–March; DJFM) SLP, SAT, precipitation and sea ice are calculated for selected periods in the observations and *Hist-assim* simulations. The observed and *Hist-assim* trends are influenced by both external forcings and internal variability. To assess which of these factors are most responsible for the pattern of trends in the model, results are also calculated for the ensemble mean of the *Hist* simulation (which will be predominately driven by external forcings) and the mean of the five strongest periods of increasing and decreasing NAO from the *piControl* simulations (which will show the influence of the NAO without any external forcing). The five periods from piControl are chosen to be independent of each other, so once a period is chosen, subsequent periods are selected such that they do not contain any overlapping years. We note however that this comparison does not allow for externally forced NAO trends that are not captured correctly by the model [6].

We also examine the influence of the NAO as well as the AMOC on the North Atlantic and in particular on SST averaged over the subpolar gyre (SPG) region. The AMOC is defined as the maximum overturning streamfunction value in the North Atlantic and is only calculated for the model simulations. The SPG region south of Greenland is defined following Caesar *et al* [33] (shown later in figure 2). For the observations this is calculated using data from HadSST4, which we only use after 1873 when data coverage in the region increases from approximately 50% to over 85%.

To examine a possible link between the NAO on the SPG we regress a time series constructed from the NAO index onto the SPG SST using a total least squares regression to calculate an estimate of the change in temperature per unit change in the NAO. To determine the contribution of this interannual effect on the SST of this region, the NAO timeseries was then multiplied by the calculated regression coefficient, in a method similar to Iles and Hegerl [3].

3. Results

3.1. Multi-decadal trends in the NAO

During the 20th Century the NAO timeseries displays substantial multi-decadal variability including periods of large positive and negative trends (figure 1(a)). To investigate the effect of these trends on Northern Hemisphere climate we concentrate on the 28 year periods of strongest positive (1963–1990) and strongest negative (1920–1947) NAO trends. The equivalent trends from the *Hist* ensemble, calculated over the same periods (to account for any externally forced component) are much smaller than those observed (circles top figure 1(b)). This is also the case for nearly all CMIP6 model simulations analysed (figure 1(b), 187 simulations in total), nearly all periods of unforced variability in the piControl simulations (see figure S2) and is consistent with results from CMIP5 [9]. While this comparison focuses on 28 years (a similar time period to Bracegirdle *et al* [9] and Eade *et al* [10] who analysed 30 year periods), other time periods show similar discrepancies between models and observations (see figures S3–S5). This suggests that the model simulations used either do not capture the long-term NAO variability, or the NAO response to forcing or both. Equally, no CMIP6 projections of the near-term future (the period 2023–2050) contain 28 year trends as large as these two observed extremes (figure 1(b), 306 simulations in total), meaning that if these past trends were to reoccur, they would lie outside the range of possible future climates as simulated by present-day climate models [16]. This potentially represents a problem for policy makers and other users of climate predictions who require reliable uncertainty estimates, and highlights the need for further work to understand the causes of decadal variability [34, 35].

The *Hist-assim* simulation, by design, has a realistic representation of the NAO throughout this period (figure 1(a)). Thus, comparison between it, the observed variability and *Hist* can be used to investigate the effect that large multi-decadal trends in the NAO have had on Northern Hemisphere climate during particular periods in the past. While commonly assumed to be a mode of internal variability, some past work has proposed that much of the long-term variability in the NAO may be due to external forcings [6]. Although our particle filter model setup does not allow us to discriminate between a forced or internal variability signal, the technique ensures our *Hist-assim* simulation more accurately represents the evolution of the NAO regardless of its cause.

The observed trends in SLP (figures 2(a) and 3(a)) show strong NAO-like patterns in the two periods, which is expected as these periods were explicitly chosen as those with the strongest negative and positive NAO trends. By design the particle filter simulations also show very similar strong NAO-like behaviour in the spatial trends for these two periods (figures 2(d) and 3(d)), which demonstrates that they can be used to determine the effect of the large NAO trends on other variables. The *Hist* ensemble mean results (figures 2(g) and 3(g)) do not show any large trends indicating that the driving factor over these ~30 year time-scales is most likely dominated by internal variability (at least in the model simulations),

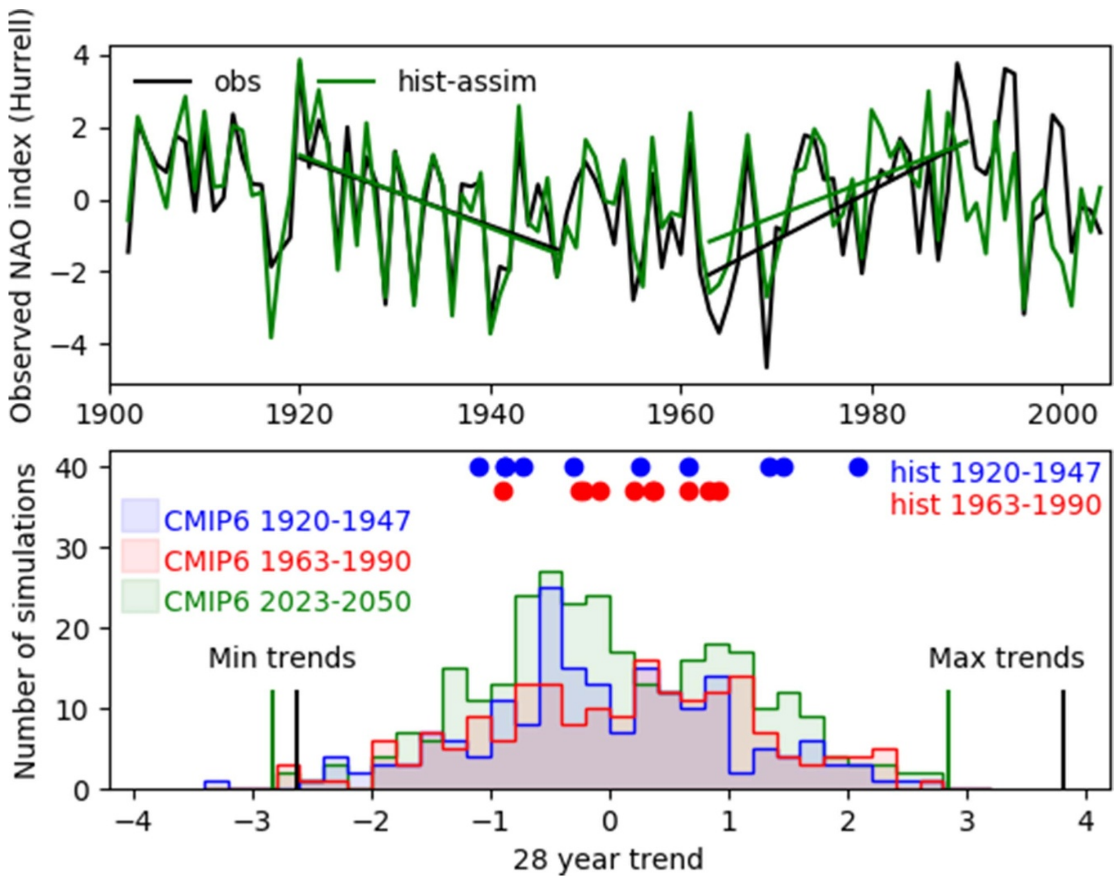

Figure 1. NAO trends in observations and model simulations. (a) Observed NAO Index (DJFM, Hurrell index, 20CRv3, black) and NAO index in *Hist-assim* simulation (green). Maximum and minimum 28 year trend shown (note downward trends in observations and simulations overlap). (b) Observed and assimilated model 28 year trends for the two periods (vertical lines). Histograms of trends for all CMIP6 simulations for the period corresponding to the maximum negative trend in observations (1920–1947 light blue histogram), maximum positive trend (1963–1990 pink histogram) and all SSP simulations for the near-term future (2015–2042 green histogram). The values for the 10 simulations without assimilation (hist) are shown by circles for 1963–1990 (red) and 1920–1947 (blue).

with external forcings playing a small role (although we cannot exclude errors in the modelled response to external factors).

For winter temperature, the trends simulated by *Hist-assim* (figures 2(e) and 3(e)) are very similar to those observed (figures 2(b) and 3(b)); with warming over northern Eurasia, cooling over southern Eurasia and warming over much of North America associated with the positive NAO trend and the opposite for the negative trend, in agreement with previous studies [3, 6]. The similarity to the 28 year trend patterns associated with strong NAO trends in the *piControl* simulations strongly support the NAO as the main driver on these multi-decadal time-scales. In key regions, the trends caused by the NAO are much stronger than the external forced trends simulated by this model, demonstrating the important role of the NAO on Northern Hemisphere winter temperature on multi-decadal timescales; for example, much of northern Europe and northern America show temperature trends at least five times stronger in the assimilated run than the ensemble mean without assimilation over the period 1963–1990 (see figure S6). This supports studies that have found that NAO variability has potential to enhance or mask global warming [4].

The *Hist-assim* precipitation trends are also very similar to observations and are much stronger than the forced trend simulated by this model (shown by the *Hist* ensemble mean). Model simulations have been found to have difficulty capturing the precipitation trends in Europe during the latter part of the 20th century [13] which highlights the importance of correctly accounting for this mode of variability. The pattern is consistent with NAO responses found previously [3, 4, 6] with an increase in precipitation in northern Europe and a drying in the Mediterranean for the period of positive NAO trend, with an opposite pattern during the period of negative NAO trend. The winter NAO has also been linked to changes in the winter monsoon over both northern India [36] and East Asia [37, 38], and long-term trends in the NAO have been associated with climate variability over China [38] and over the Tibetan Plateau [39]. Our study provides further evidence for this link since there are consistent trends in precipitation in both models and observations during the long-term increase in NAO, with increasing precipitation over

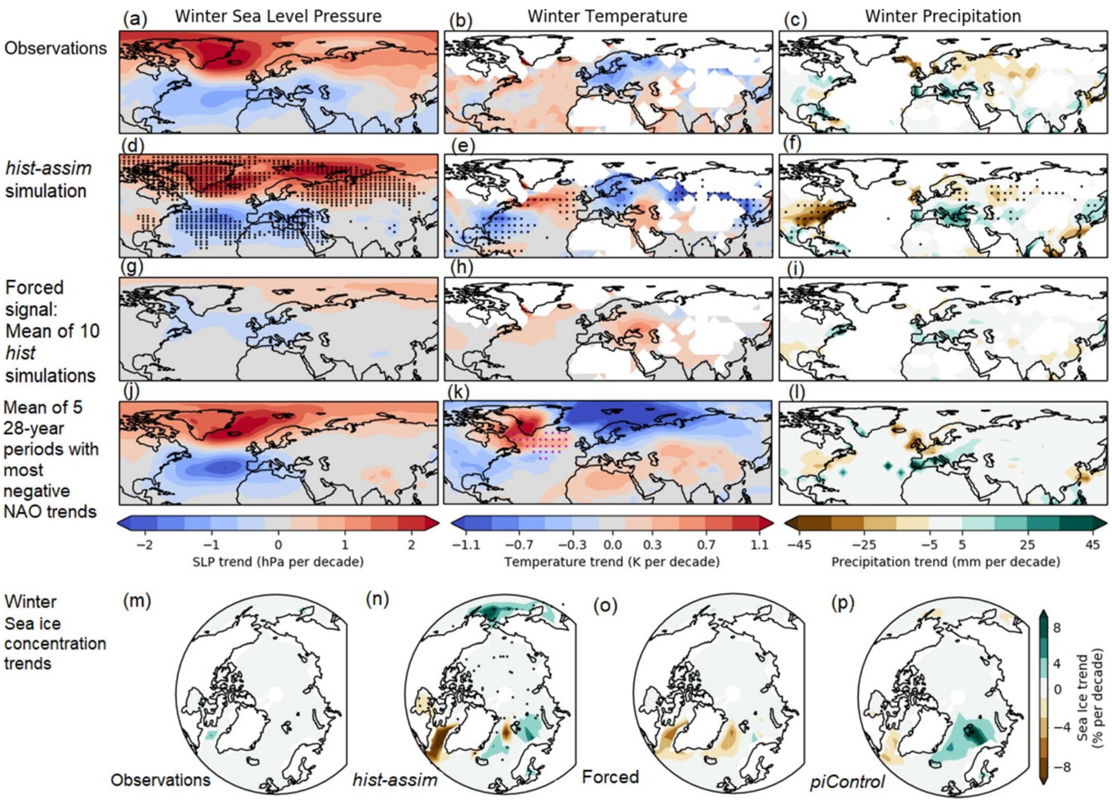

Figure 2. Effect of large negative NAO trend on winter climate. Trends during the period 1920–1947 (corresponding to the 28 year period of largest negative NAO trend), in winter (DJFM) sea-level-pressure, temperature, precipitation and annual sea ice cover. Black stippling indicates where assimilated trends are larger/smaller than all 10 of the all-forced simulations. White on the temperature panels indicates missing data. Purple stippling in panel (k) shows the SPG region.

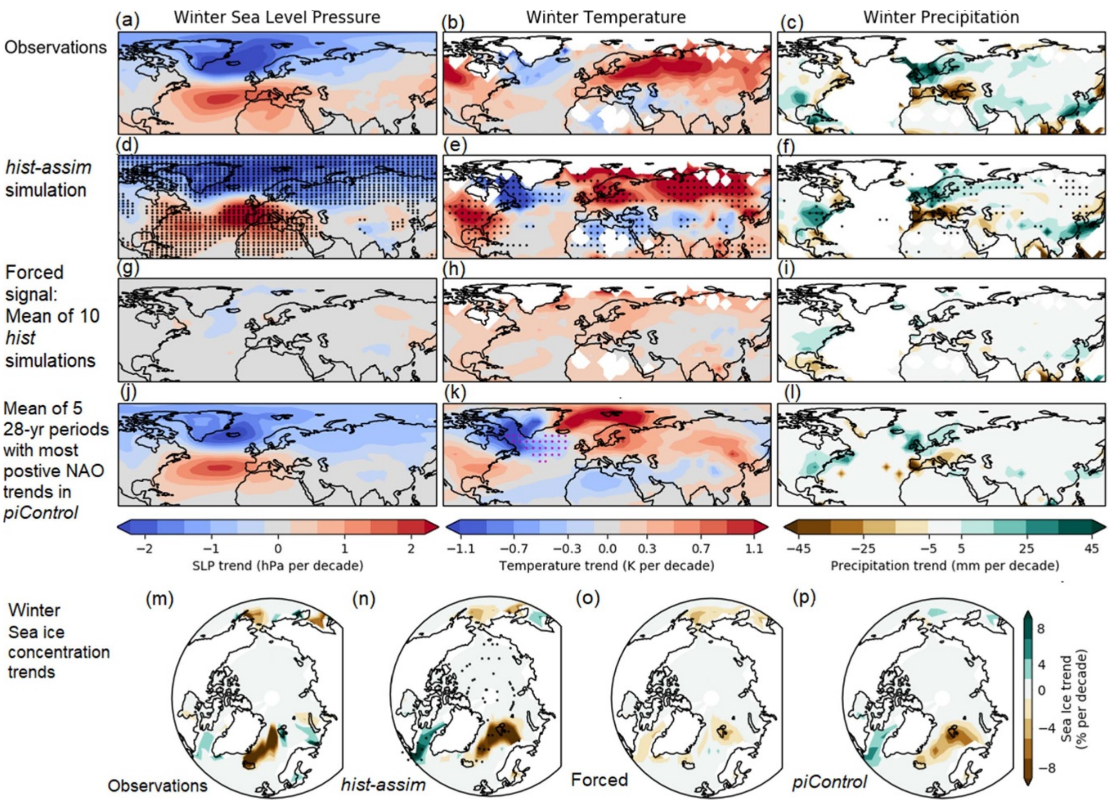

Figure 3. Effect of large positive NAO trend on winter climate. As in figure 2 but for the period 1963–1990 (corresponding to the 28 year period of largest NAO trend).

northern India and East Asia. An equivalent increase is also found in the *piControl* simulations during periods of strong NAO trends, which reinforces the evidence of an NAO link.

Simulated annual sea ice trends also show a clear NAO fingerprint, with the period of increasing NAO leading to a decrease in sea ice in the Greenland and Barents Sea, and an increase in the Labrador Sea (figure 3). The pattern reverses during periods of negative trends in NAO phase (figure 2). These trends are consistent with that expected due to an NAO influence [40]. Furthermore, by comparing the periods of maximum NAO trends in the *piControl* simulations it can be seen that the NAO is the primary driver of trends during these two 28 year periods. The observed sea-ice trends are less clear particularly during the early period (figure 2), which is to be expected given that much of the data is infilled based on sparse observational data coverage and climatology [20]. For the positive trend period (1963–1990), the observed sea-ice is based on more observations so is likely more reliable.

To investigate the persistence of the effect of the Winter NAO on the subsequent months of the year, we have investigated the 28 year trends in the period 1963–1990 in late spring (April and May), a period in which the NAO is not assimilated (figure S7). The effect of the winter NAO is clearest in the sea ice with similar trends to those seen in winter persisting in both the model simulations and the observations. Consistent tends can also be found in Atlantic SSTs in agreement with previous studies [41].

3.2. Link between the NAO, North Atlantic and AMOC

The North Atlantic SPG is an area which is strongly effected by the NAO (see figures 2–4). In this region a positive correlation (0.41) is found between the annual mean SST in *Hist-assim* and observations (figure 4(a)), which is higher than that between the observations and any *Hist* simulation (which range from −0.22 to 0.26). Given that the only difference between the two experimental set-ups is the assimilated modes, this improved agreement is very likely caused by the NAO, since the other modes are not expected to affect this region strongly and all model simulations are driven by the same forcings. The assimilated winter NAO (DJFM) was found to be anti-correlated with the annual SPG SST in both the observations (correlation = −0.33) and the *Hist-assim* simulation (correlation = −0.42), which could at least partly explain the similarities between the simulated and observed SPG timeseries. If the interannual NAO contribution is removed, as described in section 2.3, there is still decadal variability in common (correlation = 0.31; figure S10) suggesting that the effect of the NAO must also be acting on timescales longer than a year, for example due to persistence in the oceans mixed layer [42, 43]. By subtracting the forced variability as represented by the *Hist* ensemble mean from both observations and Hist-assim an estimate of the unforced SPG SST variability can be derived. On multi-decadal scales the NAO can explain much of the variability found in this region (figure 4(b)), further supporting an important role of the NAO.

In addition to the effect of multi-decadal NAO variability, the North Atlantic is also known to be influenced by large-scale ocean dynamics, particularly the AMOC, with a decreasing strength of the AMOC causing reduced northward heat transport and consequently a cooling in the SPG region [33]. The AMOC in turn can be influenced by the NAO [44, 45]. Instrumental multi-decadal measurements of the AMOC do not exist, with continuous observations by the RAPID array at 26°N only available since 2004 [46], but some longer term reconstructions use the SPG index as a proxy for changes in the AMOC [33]. The particle filter set-up is ideal for analysing these interdependencies, and the relationship between the NAO and Atlantic SPG SST as well as the AMOC over the observed period. By analysing the *Hist* ensemble and an ensemble of individually forced simulations (see section 2.2), we can determine both the effect of the total forcing on the AMOC as well as the contribution of different forcings. The combined forced variability in the *Hist* simulation shows an AMOC increase to the mid-19th Century followed by a gradual decline to a minimum at the start of the 20th Century with a subsequent recovery to another maximum at the end of the 20th Century (figure 4(c)). This is reflected in the forced variability in the simulated annual mean SPG SST, which follows a very similar low frequency evolution (correlation coefficient of 0.73, increasing to 0.79 if the SPG lags the AMOC by 7 years).

Volcanic eruptions appear responsible for the largest pre-industrial changes in the AMOC (figures 4(d) and S8), consistent with previous studies [47–50]. An epoch analysis where the average change of the AMOC following an eruption is calculated, shows that in our simulations there is a statistically significant increase in the AMOC a decade after a large eruption followed by a decrease in the AMOC approximately 40 years after the eruption (figure S9). The effect of anthropogenic forcing is broadly consistent with that found recently for a much larger ensemble of CMIP6 simulations [51] (although the amplitude of simulated change is weaker than the multi-model CMIP6 mean), with GHGs driving a steady decrease in the AMOC since approximately the start of the 20th Century, offset by anthropogenic aerosols which cause the AMOC to increase.

For *Hist-assim* (figure 4(e)), results are from a single simulation, so more internal variability (including due to the NAO) can be expected compared to the *Hist* ensemble mean (which

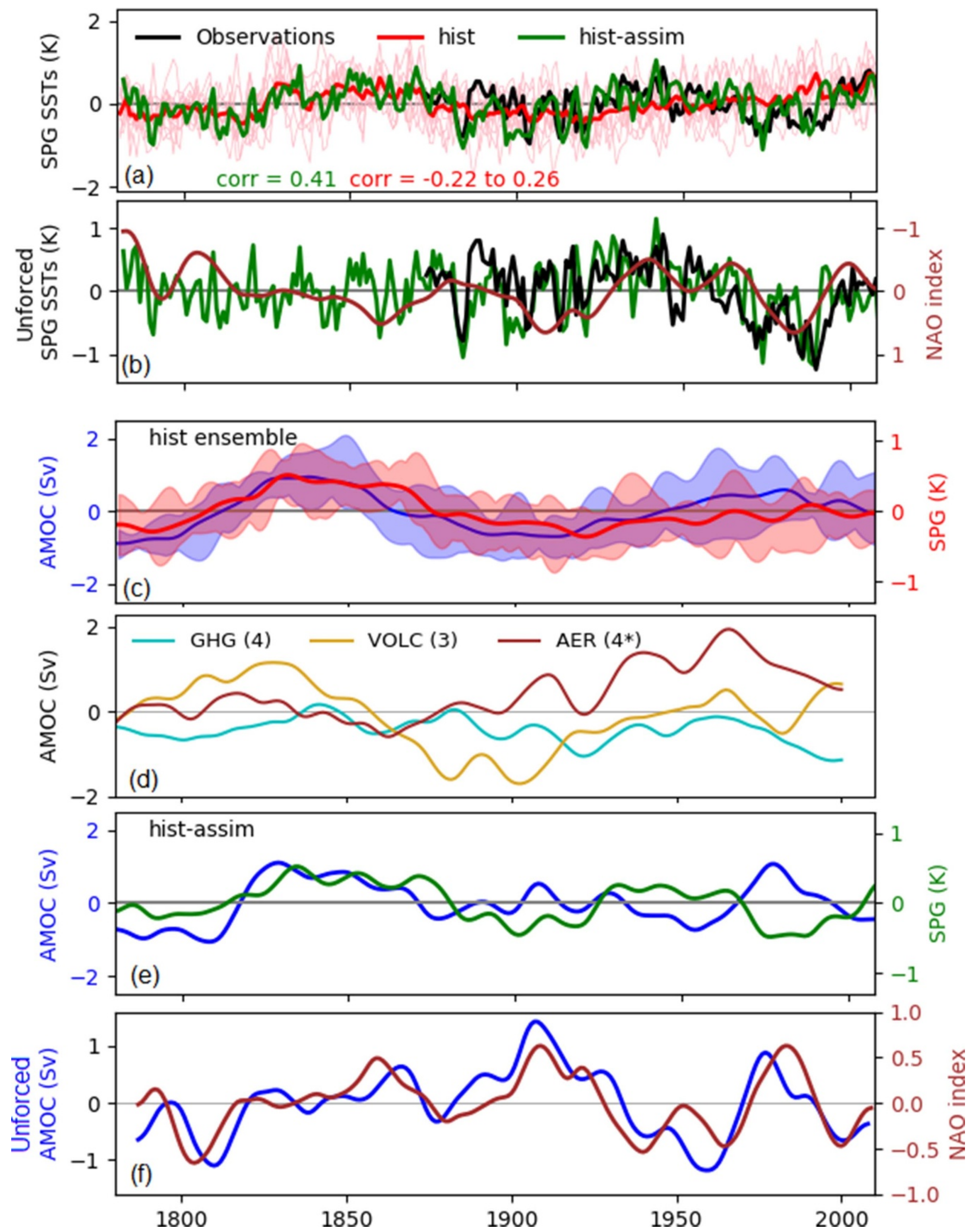

Figure 4. Subpolar gyre SST, NAO and AMOC. (a) Annual mean SST in the subpolar gyre. Pink: *Hist* simulations with ensemble mean (red). Green: *Hist-assim*. Black: observations. (b) SST in the subpolar gyre with forced component (*Hist* ensemble mean) removed, Black: observations. Green: *Hist-assim*, compared to NAO in *Hist-assim* (brown) (c) *Hist* ensemble mean and spread for AMOC (blue) and SPG SST (red) (d) AMOC from the ensemble mean of individually forced simulations (number in brackets indicates the number of simulations averaged, with the aerosol response calculated as the mean of 4 All forced simulations minus 4 simulations with all forcings except aerosol). (e) AMOC (blue) and SPG SST (green) for *Hist-assim*. (f) AMOC for *Hist-assim* with forced component (*Hist* ensemble mean) removed (blue), compared to its NAO index (brown). All data except SPG SSTs in panels (a) and(b) low-passed filtered by a 10 year Butterworth filter.

emphasises the externally forced component simulated by this model). The *Hist-assim* AMOC shares some characteristics with the ensemble mean, on very low frequencies; in particular, the volcanically forced strong AMOC during the middle of the 19th Century, which is also reflected in a warmer SPG during this period. The similarity to the NAO timeseries on multi-decadal timescales strongly suggests that the non-forced signal in *Hist-assim* AMOC is dominated by the NAO (figure 4(f)). A similar response of the AMOC to periods of strong NAO was also found by Delworth *et al* [7, 44] who, by prescribing heat fluxes to the SPG region mimicking the effect of the NAO, concluded that a positive phase of the NAO strengthens the AMOC by increasing deep water formation in the North Atlantic and thus horizontal density gradients. Although the low-pass filtering makes it complicated to determine which component (the AMOC or the SPG) leads which, crucially due to the particle filtering set-up, the NAO is forced to follow the observed timeseries, so that any effect of the AMOC on the NAO will be suppressed on these timescales. Hence, in this set-up, such a close relationship must be due to the NAO driving the AMOC (rather than the other way around). These results suggest that the NAO could lead to predictability on decadal timescales through changes to the AMOC, and the AMOC variability simulated is consistent with experiments using decadal forecast simulations that have found that initializing simulations in the 1960s with a weak AMOC can lead to skilful predictions of the exceptionally cold period observed in the 1960s and 1970s [32] and that initializing with a stronger AMOC in the 1980s can predict the subsequent warm SPG [52].

One important point to note is that although the AMOC timeseries is positively correlated with the SPG SST in the *Hist* ensemble mean (as expected from previous work [33]; figure 4(c)) and on very long timescales in *Hist-assim* (figure 4(e)) it is actually anti-correlated in *Hist-assim* on shorter (decadal to multi-decadal) timescales. This can be explained due to the effect of the NAO on both the SPG SSTs (anti-correlation, which can be seen in figures 2, 3 and 4(b)) and the AMOC (positive correlation), which results is an apparent anti-correlation between the AMOC and SPG on multi-decadal scales.

While assimilating the NAO significantly improves the agreement with the observed SPG SST timeseries and the northern most part of the Atlantic, the same is not true for the rest of the Atlantic (see figure S11 and Schurer *et al* [27]) and *Hist-assim* does not agree with the observed AMV which represents the average anomalies of the whole North Atlantic basin. The evolution of SST in this region has been attributed to external forcings [8, 53–56], so the disagreement between the observations and model could be due to deficiencies in the model's response to forcing (for example the relatively crude treatment of anthropogenic aerosols), or represent multi-decadal internal ocean variability. The response of the AMOC to the NAO, as well as the effect of the AMOC on Atlantic SST, have been found to vary considerably between models [7, 8, 11]. It is thus plausible that the use of a different model would result in a different effect on the AMV, possibly closer to that observed, particularly given the ocean model used in our study is of relatively low resolution and, in common with all CMIP6 climate models, does not include an interactive ice sheet model [57].

4. Conclusions

In this study, we have analysed results from a recently published set of experiments, which uses data-assimilation techniques to produce a near-continuous model simulation with a realistic realisation of the ENSO, NAO and SAM (similar to that which actually occurred over the measurement record). This has allowed us to determine the effect, in our model, of approximately replicating the time evolution of the winter NAO. This is particularly important as the observed NAO has displayed larger multi-decadal trends in the 20th Century than in nearly all CMIP6 model simulations, so this model set-up allows us to examine the impacts of observed NAO variability and the consequence of this model deficiency in decadal atmospheric variability.

We focus our analysis on the effect of strong positive and negative NAO trends on the climate of the mid to high latitudes in the Northern Hemisphere. We found that the large NAO trends can explain the majority of the winter temporal changes in SAT, precipitation and sea-ice cover during a period of increasing NAO (1963–1990) and decreasing NAO (1920–1947), and furthermore that the effect of the NAO dominates over that of the forced trend (as simulated by our model) in regions strongly affected by the NAO. Given the potential discrepancies in long-term NAO behaviour between model simulations and observations further work is needed to understand the causes of multi-decadal NAO variability and care should be taken that NAO-induced trends are not mis-attributed to other causes.

We have further analysed changes in the SPG SST, which has been identified as a key region for Atlantic variability. A reasonably strong correlation between *Hist-assim* and the observations suggests that the simulations are capturing many of the key processes, and the higher correlation compared to any of the forcing-only (*Hist*) simulations demonstrates a significant contribution from the NAO in this region which can explain much of the SPG SST variability on annual to multi-decadal scales. Our results also suggest that variations in the AMOC cause low frequency variability in the SPG SSTs. Much of this variation is driven by external forcings, such as the effect of the strong volcanic forcing in the early part of the 19th Century, which causes a period of strong AMOC and therefore increased SPG SST towards the middle of the century. However there is also an effect of the NAO on the AMOC in the *Hist-assim* experiment driving multi-decadal variability, which appears consistent with observed SPG variability. We therefore caution against using SPG SST as an unambiguous proxy for the AMOC on less than multi-decadal timescales, and recommend that the NAO contribution should be taken into account in attribution of AMOC changes.

In this study we have demonstrated the value of using a particle-filter data-assimilation technique to investigate the effect of large multidecadal NAO variability. By only assimilating large scale modes of variability and not introducing any nudging terms the simulation outputs could be compared to model simulations without assimilation to isolate just the effect of following the observed evolution of these modes. This technique has great potential, as it allows scientists to generate model simulations that are targeted at physically plausible outcomes in different parts of the climate systems. For example, one particularly promising application could be investigating possible storylines in future climate projections, such as the potential importance of large trends in the NAO reoccurring over the next few decades.

Data availability statement

The model data that support the findings of this study are openly available. The Hist-assim simulation data is available at https://doi.org/10.7488/ds/3829. The Hist simulations at https://doi.org/10.7488/ds/3827 and the single forced HadCM3 simulations are available at the Center for Environmental Data Analysis: http://catalogue.ceda.ac.uk/uuid/b6c714aad70936d663e2e235aa91187c and CMIP6 model output is available at: https://esgf-node.llnl.gov/projects/cmip6/.

Acknowledgments

A S was funded by the ERC funded project TITAN (EC-320691), NERC under the Belmont forum, Grant PacMedy (NE/P006752/1), the NERC project GloSAT (NE/S015698/1) and received funding from a Chancellors fellowship at the University of Edinburgh. Hugues Goosse is research director at the Fonds de la Recherche Scientifique (F.R.S.-FNRS). MHE acknowledges funding from the Australian Research Council (ARC Grant ID's SR200100008, LP200100406, DP190100494). DMS was supported by the Met Office Hadley Centre Climate Programme funded by BEIS and Defra. We are grateful to the reviewers for insightful comments that have improved the manuscript and its presentation.

ORCID iDs

Andrew P Schurer https://orcid.org/0000-0002-9176-3622
Gabriele C Hegerl https://orcid.org/0000-0002-4159-1295
Hugues Goosse https://orcid.org/0000-0002-5438-3612
Massimo A Bollasina https://orcid.org/0000-0001-7509-7650
Matthew H England https://orcid.org/0000-0001-9696-2930
Doug M Smith https://orcid.org/0000-0001-5708-694X
Simon F B Tett https://orcid.org/0000-0001-7526-560X

References

[1] Hurrell J W, Kushnir Y, Ottersen G and Visbeck M 2003 An overview of the North Atlantic Oscillation *Geophys. Monogr. Ser.* **134** 1–35
[2] Wallace J M, Fua Q, Smoliaka B V, Lina P and Johansona C M 2012 Simulated versus observed patterns of warming over the extratropical Northern Hemisphere continents during the cold season *Proc. Natl Acad. Sci. USA* **109** 14337–42
[3] Iles C and Hegerl G 2017 Role of the North Atlantic Oscillation in decadal temperature trends *Environ. Res. Lett.* **12** 114010
[4] Deser C, Hurrell J W and Phillips A S 2017 The role of the North Atlantic Oscillation in European climate projections *Clim. Dyn.* **49** 3141–57
[5] Deser C, Phillips A S, Alexander M A and Smoliak B V 2014 Projecting North American climate over the next 50 years: uncertainty due to internal variability *J. Clim.* **27** 2271–96
[6] Smith D M *et al* 2020 North Atlantic climate far more predictable than models imply *Nature* **583** 796–800
[7] Delworth T L, Zeng F, Zhang L, Zhang R, Vecchi G A and Yang X 2017 The central role of ocean dynamics in connecting the North Atlantic Oscillation to the extratropical component of the Atlantic multidecadal oscillation *J. Clim.* **30** 3789–805
[8] Zhang R, Sutton R, Danabasoglu G, Kwon Y O, Marsh R, Yeager S G, Amrhein D E and Little C M 2019 A review of the role of the Atlantic meridional overturning circulation in Atlantic multidecadal variability and associated climate impacts *Rev. Geophys.* **57** 316–75
[9] Bracegirdle T J, Lu H, Eade R and Woollings T 2018 Do CMIP5 models reproduce observed low-frequency North Atlantic jet variability? *Geophys. Res. Lett.* **45** 7204–12
[10] Eade R, Stephenson D B, Scaife A A and Smith D M 2022 Quantifying the rarity of extreme multi-decadal trends: how unusual was the late twentieth century trend in the North Atlantic Oscillation? *Clim. Dyn.* **58** 1555–68
[11] Ba J 2014 A multi-model comparison of Atlantic multidecadal variability *Clim. dyn.* **43** 2333–48
[12] Simpson I R, Deser C, McKinnon K A and Barnes E A 2018 Modeled and observed multidecadal variability in the North Atlantic jet stream and its connection to sea surface temperatures *J. Clim.* **31** 8313–38
[13] Blackport R and Fyfe J C 2022 Climate models fail to capture strengthening wintertime North Atlantic jet and impacts on Europe *Sci. Adv.* **8** 3112
[14] Omrani N E, Keenlyside N S, Bader J and Manzini E 2014 Stratosphere key for wintertime atmospheric response to warm Atlantic decadal conditions *Clim. Dyn.* **42** 649–63
[15] Hardiman S C, Dunstone N J, Scaife A A, Smith D M, Comer R, Nie Y and Ren H-L 2022 Missing eddy feedback may explain weak signal-to-noise ratios in climate predictions *npj Clim. Atmos. Sci.* **5** 1–8
[16] O'Reilly C H, Befort D J, Weisheimer A, Woollings T, Ballinger A and Hegerl G 2021 Projections of northern hemisphere extratropical climate underestimate internal variability and associated uncertainty *Commun. Earth Environ.* **2** 1–9
[17] Morice C P, Kennedy J J, Rayner N A, Winn J P, Hogan E, Killick R E, Dunn RJ, Osborn TJ, Jones PD and Simpson IR 2021 An updated assessment of near-surface temperature

change from 1850: the HadCRUT5 data set *J. Geophys. Res.* **126** e2019JD032361
[18] Kennedy J J, Rayner N A, Atkinson C P and Killick R E 2019 An ensemble data set of sea surface temperature change from 1850: the met office Hadley Centre HadSST.4.0.0.0 data set *J. Geophys. Res.* **124** 7719–63
[19] Slivinski L C *et al* 2021 An evaluation of the performance of the twentieth century reanalysis version 3 *J. Clim.* **34** 1417–38
[20] Titchner H A and Rayner N A 2014 The met office Hadley Centre sea ice and sea surface temperature data set, version 2: 1. Sea ice concentrations *J. Geophys. Res.* **119** 2864–89
[21] Schneider U, Ziese M, Meyer-Christoffer A, Finger P, Rustemeier E and Becker A 2016 The new portfolio of global precipitation data products of the global precipitation climatology centre suitable to assess and quantify the global water cycle and resources *Proc. IAHS* **374** 29–34
[22] Pope V D, Gallani M L, Rowntree P R and Stratton R A 2000 The impact of new physical parametrizations in the Hadley Centre climate model: HadAM3 *Clim. Dyn.* **16** 123–46
[23] Gordon C, Cooper C, Senior C A, Banks H, Gregory J M, Johns T C, Mitchell J F B and Wood R A 2000 The simulation of SST, sea ice extents and ocean heat transports in a version of the Hadley Centre coupled model without flux adjustments *Clim. Dyn.* **16** 147–68
[24] Schurer A P, Tett S F B and Hegerl G C 2014 Small influence of solar variability on climate over the past millennium *Nat. Geosci.* **7** 104–8
[25] Brönnimann S *et al* 2019 Last phase of the Little Ice Age forced by volcanic eruptions *Nat. Geosci.* **12** 650–6
[26] Schurer A, Mineter M and Tett S 2023 10 member ensemble of HadCM3 simulations, 1780-2009 [dataset] (University of Edinburgh, School of GeoSciences) (https://doi.org/10.7488/ds/3827)
[27] CPD Quantifying the contribution of forcing and three prominent modes of variability on historical climate 2022 (available at: https://cp.copernicus.org/preprints/cp-2022-55/)
[28] Schurer A, Mineter M, Hegerl G, Goosse H, Bollasina M, England M, Smith D and Tett S 2023 Particle filter HadCM3 simulation, 1781-2008 [dataset] (University of Edinburgh, School of GeoSciences) (https://doi.org/10.7488/ds/3829)
[29] Goosse H, Crespin E, Dubinkina S, Loutre M F, Mann M E, Renssen H, Sallaz-Damaz Y and Shindell D 2012 The role of forcing and internal dynamics in explaining the 'medieval climate anomaly' *Clim. Dyn.* **39** 2847–66
[30] Dubinkina S, Goosse H, Sallaz-Damaz Y, Crespin E and Crucifix M 2011 Testing a particle filter to reconstruct climate changes over the past centuries *Int. J. Bifurcation Chaos* **21** 3611–8
[31] Luterbacher J *et al* 2001 Extending North Atlantic Oscillation reconstructions back to 1500 *Atmos. Sci. Lett.* **2** 114–24
[32] Robson J, Sutton R and Smith D 2014 Decadal predictions of the cooling and freshening of the North Atlantic in the 1960s and the role of ocean circulation *Clim. Dyn.* **42** 2353–65
[33] Caesar L, Rahmstorf S, Robinson A, Feulner G and Saba V 2018 Observed fingerprint of a weakening Atlantic Ocean overturning circulation *Nature* **556** 191–6
[34] Smith D M *et al* 2022 Attribution of multi-annual to decadal changes in the climate system: the large ensemble single forcing model intercomparison project (LESFMIP) *Front. Clim.* **4** 146
[35] Findell K L *et al* 2022 Explaining and predicting earth system change: a world climate research programme call to action *Bull. Am. Meteorol. Soc.* **104** E325–39
[36] Midhuna T M and Dimri A P 2019 Impact of arctic oscillation on Indian winter monsoon *Meteorol. Atmos. Phys.* **131** 1157–67
[37] Bollasina M A and Messori G 2018 On the link between the subseasonal evolution of the North Atlantic Oscillation and East Asian climate *Clim. Dyn.* **51** 3537–57
[38] He S, Gao Y, Li F, Wang H and He Y 2017 Impact of Arctic Oscillation on the East Asian climate: a review *Earth-Sci. Rev.* **164** 48–62
[39] Li J, Yu R and Zhou T 2008 Teleconnection between NAO and climate downstream of the Tibetan Plateau *J. Clim.* **21** 4680–90
[40] Deser C, Walsh J E and Timlin M S 2000 Arctic sea ice variability in the context of recent atmospheric circulation trends *J. Clim.* **13** 617–33
[41] Herceg-Bulić I and Kucharski F 2014 North Atlantic SSTs as a link between the wintertime NAO and the following spring climate *J. Clim.* **27** 186–201
[42] Coëtlogon G and Frankignoul C 2003 The persistence of winter sea surface temperature in the North Atlantic *J. Clim.* **16** 1364–77
[43] Cassou C, Deser C and Alexander M A 2007 Investigating the impact of reemerging sea surface temperature anomalies on the winter atmospheric circulation over the North Atlantic *J. Clim.* **20** 3510–26
[44] Delworth T L and Zeng F 2016 The impact of the North Atlantic Oscillation on climate through its influence on the Atlantic meridional overturning circulation *J. Clim.* **29** 941–62
[45] Danabasoglu G, Yeager S G, Kwon Y O, Tribbia J J, Phillips A S and Hurrell J W 2012 Variability of the Atlantic meridional overturning circulation in CCSM4 *J. Clim.* **25** 5153–72
[46] McCarthy G D, Smeed D A, Johns W E, Frajka-Williams E, Moat B I, Rayner D, Baringer M O, Meinen C S, Collins J and Bryden H L 2015 Measuring the Atlantic meridional overturning circulation at 26°N *Prog. Oceanogr.* **130** 91–111
[47] Otterå O H, Bentsen M, Drange H and Suo L 2010 External forcing as a metronome for Atlantic multidecadal variability *Nat. Geosci.* **3** 688–94
[48] Swingedouw D, Ortega P, Mignot J, Guilyardi E, Masson-Delmotte V, Butler P G, Khodri M and Séférian R 2015 Bidecadal North Atlantic ocean circulation variability controlled by timing of volcanic eruptions *Nat. Commun.* **6** 1–12
[49] Swingedouw D, Mignot J, Ortega P, Khodri M, .Menegoz M, Cassou C and Hanquiez V 2017 Impact of explosive volcanic eruptions on the main climate variability modes *Glob. Planet. Change* **150** 24–45
[50] Pausata F S R, Chafik L, Caballero R and Battisti D S 2015 Impacts of high-latitude volcanic eruptions on ENSO and AMOC *Proc. Natl Acad. Sci. USA* **112** 13784–8
[51] Menary M B *et al* 2020 Aerosol-forced AMOC changes in CMIP6 historical simulations *Geophys. Res. Lett.* **47** e2020GL088166
[52] Yeager S G, Karspeck A R and Danabasoglu G 2015 Predicted slowdown in the rate of Atlantic sea ice loss *Geophys. Res. Lett.* **42** 10704–13
[53] Undorf S, Bollasina M A, Booth B B B and Hegerl G C 2018 Contrasting the effects of the 1850–1975 increase in sulphate aerosols from North America and Europe on the Atlantic in the CESM *Geophys. Res. Lett.* **45** 11930–40
[54] Booth B B B, Dunstone N J, Halloran P R, Andrews T and Bellouin N 2012 Aerosols implicated as a prime driver of twentieth-century North Atlantic climate variability *Nature* **484** 228–32
[55] Murphy L N, Bellomo K, Cane M and Clement A 2017 The role of historical forcings in simulating the observed Atlantic multidecadal oscillation *Geophys. Res. Lett.* **44** 2472–80
[56] Watanabe M and Tatebe H 2019 Reconciling roles of sulphate aerosol forcing and internal variability in Atlantic multidecadal climate changes *Clim. Dyn.* **53** 4651–65
[57] Swingedouw D, Houssais M N, Herbaut C, Blaizot A C, Devilliers M and Deshayes J 2022 AMOC recent and future trends: a crucial role for oceanic resolution and Greenland melting? *Front. Clim.* **4** 32